frontiers in Earth Science

ORIGINAL RESEARCH
published: 31 July 2018
doi: 10.3389/feart.2018.00094

Paraglacial Rock Slope Adjustment Beneath a High Mountain Infrastructure—The Pilatte Hut Case Study (Écrins Mountain Range, France)

Pierre-Allain Duvillard[1,2]*, *Ludovic Ravanel*[1,3], *Philip Deline*[1] and *Laurent Dubois*[4]

[1] Univ. Grenoble Alpes, Univ. Savoie Mont Blanc, CNRS, EDYTEM, Chambéry, France, [2] IMSRN, Parc Pré Millet, Montbonnot, France, [3] Scientific Council of the Fédération Française des Clubs Alpins et de Montagne, Paris, France, [4] CEREMA, Direction territoriale Centre-Est, RRMS/Risques, Bron, France

Landslides triggered by shrinking glaciers are an expected outcome of global climate change and they pose a significant threat to inhabitants and infrastructure in mountain valleys. In this study we document the rock slope movement that has affected the Pilatte hut (2,572 m a.s.l.) in the Écrins range (French alps) since the 1980s. We reconstructed the geometry of the unstable rock mass using Terrestrial Laser Scanning and quantified the unstable volume (~400,000 m^3). Field observations and annual crack surveys have been used to identify the dynamics of past movements. These movements initiated in the late 1980s and have accelerated since 2000. The current trend seems to be toward a relative stabilization. Reconstruction of the glacier surface using past images taken since 1960 and "Structure from Motion" photogrammetry showed that the glacier probably applied stresses to the rock slope during its short-lived advance during the 1980s, followed by debuttressing caused by rapid surface lowering until the present day. The relationship between observed crack propagation and glacier surface change suggests that the rock slope instability is a paraglacial response to glacier surface changes, and highlights that such responses can occur within a decade of glacier change.

Keywords: rock slide, paraglacial processes, glacier retreat, Terrestrial Laser Scanning, crack-meters, high mountain infrastructure, Écrins range

OPEN ACCESS

Edited by:
Mark Naylor,
University of Edinburgh,
United Kingdom

Reviewed by:
Lindsey Isobel Nicholson,
Universität Innsbruck, Austria
Emanuele Intrieri,
Università di Firenze, Italy

***Correspondence:**
Pierre-Allain Duvillard
pierre-allain.duvillard@univ-smb.fr

Specialty section:
This article was submitted to Geohazards and Georisks, a section of the journal Frontiers in Earth Science

Received: *28 February 2018*
Accepted: *22 June 2018*
Published: *31 July 2018*

Citation:
Duvillard P-A, Ravanel L, Deline P and Dubois L (2018) Paraglacial Rock Slope Adjustment Beneath a High Mountain Infrastructure—The Pilatte Hut Case Study (Écrins Mountain Range, France). Front. Earth Sci. 6:94. doi: 10.3389/feart.2018.00094

INTRODUCTION

Temperatures in the French Alps have risen by 1.5–1.8°C since 1950 (Einhorn et al., 2015). Above 4,000 m a.s.l., the mean annual air temperature increased by 0.14°C per decade between 1900 and 2004 (Gilbert and Vincent, 2013). High alpine environments are strongly affected by this warming (Beniston et al., 2018), especially with regards to glacial shrinkage (Vincent, 2002) and permafrost degradation (Harris et al., 2009). In the Alps, the glacierized areas shrank by half between 1860 and 2012, with a strong acceleration in recession since the 1980s (Huss, 2012; Gardent et al., 2014). Mountain permafrost, defined as ground that remains below 0°C for 2 years or more, has experienced an almost continuous warming (PERMOS, 2016) since the beginning of the 2000s.

The paraglacial concept proposed by Church and Ryder (1972) describes the non-glacial processes directly conditioned by glaciation, as well as the period over which paraglacial processes are operating (Ballantyne, 2002, 2013; Mercier, 2008; Cossart et al., 2013). Deglaciation periods generally correspond to periods of intense geomorphological change, sometimes called "paraglacial morphogenic crisis" (Mercier, 2010), and these trigger significant natural destructive events (Deline et al., 2012). Widespread glacial shrinkage causes localized changes in the stress regime of the adjacent valley flanks which may cause deep-seated mass movements of rock (landslides) (O'Connor and Costa, 1993; Blair, 1994; Haeberli et al., 1997; Kääb et al., 2005; Oppikofer et al., 2008). These geomorphological processes can be the source of indirect threats to valleys through cascading processes (Huggel et al., 2005), or direct threats to mountaineers (Ritter et al., 2012; Mourey and Ravanel, 2017) and infrastructure built on moraines and rock slopes (Strozzi et al., 2010; Ravanel et al., 2015b; Kos et al., 2016).

Our understanding of the theoretical mechanics of paraglacial rock slope instabilities and their drivers (McColl, 2012) is being continually improved through detailed case studies (e.g., Wieczorek and Jäger, 1996; Cossart et al., 2008; Krautblatter and Leith, 2015). The response time for triggering paraglacial instability of rock slopes after the deglaciation period can be ten to one hundred years (Ballantyne, 2002), although this remains poorly documented due to the difficulty in anticipating this process (Zanoner et al., 2017). Examples of infrastructure built on potentially paraglacial unstable rock slopes are rare (Duvillard et al., 2015) but offer reliable cases to document the slope response in the initial years after de-icing. At least three infrastructure are known to have been affected by paraglacial rock slides during the last two decades: the *Gletscherbahn Moosfluh* cable-car near the Aletsch glacier in Switzerland (Kos et al., 2016; Grämiger et al., 2017), and the Mueller (McColl and Davies, 2013) and Murchison huts in the New Zealand Alps (Petley, 2017).

This study focuses on the Pilatte hut (2,572 m a.s.l., in the Écrins mountain range, French Alps). Initial damage to the hut, in the form of small cracks, was observed in the late 1980s, but the opening of a large crack in the hut foundations and walls in the early 2000s was of great concern to its managers. The rock slope on which the hut is built, adjacent to the Pilatte glacier, has been monitored since 2003 with ground-based surveying techniques and more recently with high-resolution topographic imagery.

To test the hypothesis that the subsidence behind the damage to the Pilatte hut is a result of paraglacial slope adjustment, this research project aims to study the geometry and the dynamics of the rock mass movement and its relationship with the lowering of the Pilatte glacier surface.

STUDY SITE

The Pilatte Hut

The Pilatte hut is located on a rocky glacier-polished knoll at 2,572 m a.s.l. in the Écrins National Park, currently 270 m above the left-hand margin of the Pilatte glacier in the upper Vénéon valley (**Figure 1**). The hut, accessed by a 3h30 hike from the hamlet of La Bérarde, is managed by the *Club Alpin Français* (CAF) and has a bedding capacity of 120. It is mainly frequented by hikers and, to a lesser extent, by alpinists climbing Les Bans (3,669 m a.s.l.), Mont Gioberney (3,352 m a.s.l.) and other peaks.

A wooden hut was first built here in 1925 and is presently used as the winter hut. In 1954, the growth of mountain activities led to the construction of a larger hut with cemented stone walls. A reinforced concrete extension on the west side was built in 1994 to increase the number of beds and to improve the comfort and privacy of the hut keepers.

Geological Setting

The Écrins-Pelvoux mountain range is one of the External Crystalline Ranges of the Western Alps. The upper Vénéon valley is a classic U-shaped glacial valley with very steep, regular slopes. The ice thickness during the Last Glacial Period in the Vénéon valley likely exceeded 1,000 m (Delunel, 2010). The lithology of the knoll upon which the Pilatte hut is built is Peyre Arguet gneiss surrounded by Augen gneiss on its eastern and western sides; further west, Bérarde and Les Bans are granitic (Le Fort, 1971; Barféty and Pécher, 1984). Permafrost is absent in the surroundings of the hut because of the relatively low elevation of the area and an unfavorable geomorphological context (Marcer et al., 2017a).

The Pilatte Glacier

The hut is separated from the glacier by a very steep and partly overhanging 270 m-high rock wall, which has progressively deglaciated since the end of the Little Ice Age (LIA). The till around the hut is relatively recent and was deposed during the LIA (Vivian and Bergeret, 1967). The glacier length has decreased by *c.* 1.8 km since the LIA (Gardent et al., 2014); its mean equilibrium-line altitude rose by *c.* 300 m during the 1984–2014 period, with a mean mass balance of -1.08 m w.e a^{-1} (meters water equivalent by years) during the same period (Rabatel et al., 2013, 2016). The surface area of the glacier decreased by 11.1% between 1967–1971 and 2006–2009; 11% of its area was debris-covered in 2006–2009 (Gardent et al., 2014).

METHODS

Three different methods were used over different time periods following an initial structural and geological survey of the rock outcrop: (i) annual crack measurements were done from 2003 to 2017, and the results analyzed to detect and study the rock dynamics in progress directly beneath the Pilatte hut, (ii) Terrestrial Laser Scanning (TLS) surveys were carried out in 2014 and 2016 to assess the volume of unstable rock and to monitor any substantial geomorphological activity over that 2 year period, and (iii) Structure for Motion (SfM) photogrammetry from historical aerial photographs was carried out to measure elevation changes of the glacier surface from 1960 to 2016.

Crack Survey

Between 1985 and 1990, limited damage (small cracks/deformation of materials) was observed on the 1954

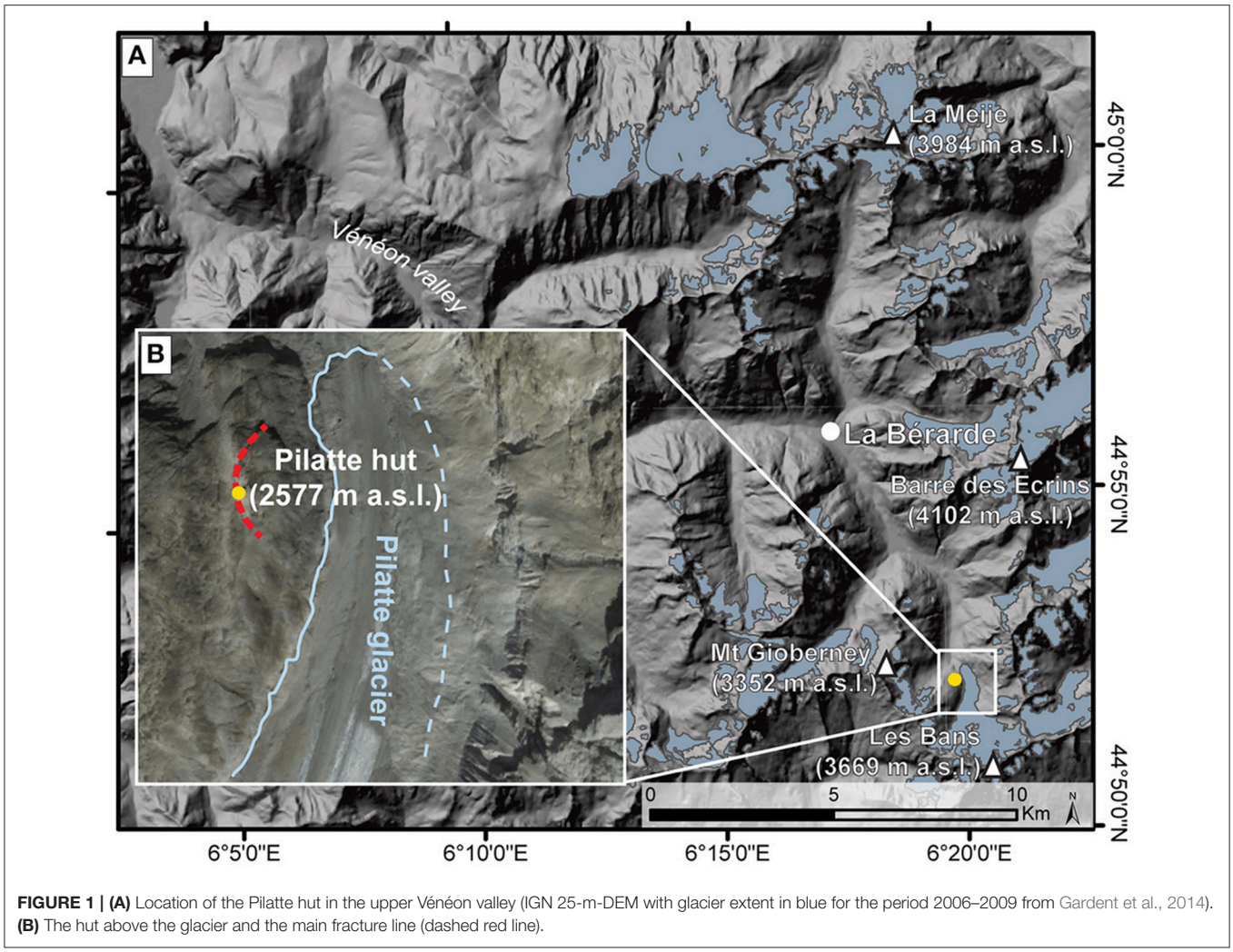

FIGURE 1 | (A) Location of the Pilatte hut in the upper Vénéon valley (IGN 25-m-DEM with glacier extent in blue for the period 2006–2009 from Gardent et al., 2014). **(B)** The hut above the glacier and the main fracture line (dashed red line).

part of the building. This became more severe between 1995 and 2000; in particular vertical cracks appeared in the north and south facades (1–2.5-cm-large) and subsidence occurred on the eastern half of the hut evidenced by the dining room floor sloping by more than 5 cm downhill, and cracks appearing in the interior walls, running from the foundations to the roof (**Figure 2**).

Since 2003, the evolution of the cracks and damage to the hut has been monitored by two structural engineering companies (initially CEBTP and then CEBEA) with 20 *Saugnac* crack-meters—a simple tool which uses a millimetric paper grid. Crack surveys are carried out three to four times during the period of opening of the hut, i.e., from April to the end of September. Data from just four gauges (numbered 7, 10, 16, and 17) were used to reconstruct the dynamic processes. These gauges had been ideally positioned, perpendicular to the main fracture line from the floor to the ceiling, and as such were deemed the most relevant.

In July 2006, a field visit was carried out to study the local structural context of the rock slope and to locate and choose the main cracks to measure annually. The major fracture lines delimiting the unstable rock mass were also surveyed annually using crack-meters (**Figure 3**). The main crack close to the hut, on the north side, was surveyed once or twice a year from 2003 to 2009 by CEBTP. In 2009, we added 8 sets of two crack-meters at the back (1), northern (2), possible downhill (3), and southern (4) limits of the rock mass which previous structural analysis had identified as being unstable (crack openings: 22.54–31.20 cm) and as evidenced by open cracks and fresh reworking of the soil. Three sets of cracks were equipped with three sets of crack-meters to measure the potential slippage and rotational dynamic of the rock mass. Since then, they have been surveyed each summer with a tape extensometer (repeatability: ±1 mm; Nordvik et al., 2010; Derron et al., 2013), or with a Vernier caliper (for the crack closest to the hut on the north side).

The main crack crossing the back of the hut (back fracture) was surveyed (dip/direction) and mapped in August 2016 by real-time kinematic dGPS *Trimble* Geo7x with 2 cm accuracy. All the crack-meters were also mapped in July 2015 by dGPS with 2 cm to 5 m accuracy (due to mask effect and low precision on the rock wall below the Pilatte hut).

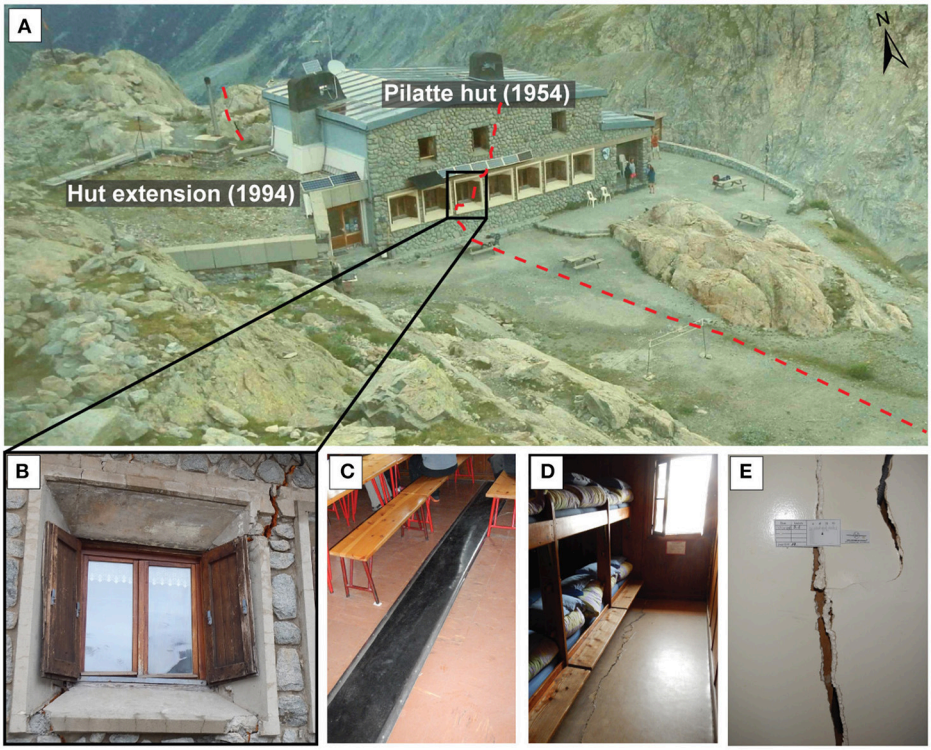

FIGURE 2 | Pilatte hut damage with main cracks shown. **(A)** The hut and the main fracture line (dashed red line). **(B)** South wall of the Pilatte hut and location of the fracture delimiting the back of the unstable rock mass in August 2016. **(C–E)** Photo taken in August 2016 of damage due to subsidence (E: *Saugnac* crack-meter).

TLS Surveys

Laser ranging is based on the transmission-reception of infrared light signals with very low spatial dispersion and high temporal precision (Slob and Hack, 2004; Telling et al., 2017). For geomorphological purposes, TLS can be used for mapping, geometry assessment or monitoring (Jaboyedoff et al., 2012; Abellan et al., 2016). Regarding the latter, some studies have been conducted in high mountain environments (Oppikofer et al., 2008, 2009; Rabatel et al., 2008; Ravanel et al., 2015a; Bhardwaj et al., 2016; Bodin et al., 2018), sometimes below infrastructure (Kenner et al., 2011; Ravanel et al., 2013, 2015b; Keuschnig et al., 2015). TLS is a very effective study method, despite certain limitations including the weight (14 kg counting the case, tripod, rotating base, laptop and generator) and cost of the equipment.

Two TLS surveys were carried out from the glacier surface to measure the entire volume of unstable terrain and to monitor the morphodynamics (rockfalls, slide) over a 2-year period. In order to carry out a kinematic survey of the rock wall below the Pilatte hut, it was scanned in July 2014 and August 2016 from two distinct positions on the glacier to avoid occlusions resulting from the complex micro-topography. To assess the unstable volume, the upper part of the rock knoll around the hut was scanned in August 2016 from six positions. An *Optech* ILRIS 3D (wavelength: 1,500 nm) was used, acquiring 2,000 pts.s^{-1} in a 40 × 40° window, with a maximum theoretical 800 m range for a reflectivity of 20–25% (the most frequent with rocks). In reality, few points are acquired beyond 500–600 m because of poor reflectivity, skewed rays, or high brightness. Our scanning was done at a maximum distance of *c.* 250 m from the rockwall. Precision in measuring a point at 100 m, and therefore the precision of the model obtained, is 7 mm for distance and 8 mm for position. Ten characteristic points such as boulders or hut corners were surveyed by dGPS in August 2016 to georeference the 3D model. The accuracy was 2–50 cm due to the masking effect of the terrain or the roof of the hut.

Cloud point alignment and georeferencing were processed using CloudCompare 2.10.V2 software (Girardeau-Montaut, 2006). Point alignment by Iterative Closest Point (ICP) algorithms (Besl and McKay, 1992; Pomerleau et al., 2013) supplied clouds of 2.105 and 20.106 × 10^6 points for 2014 and 2016, respectively.

Meshing, mapping, computing potential rock sliding volume and rockfall volumes between 2014 and 2016 were carried out with 3DReshaper software (2016 MR1 version). All the points were used for each meshing, and these were generated by a chordal deviation process with a maximum length of triangle edge of 3.5 m so as to fill the existing holes in the point clouds (zones masked by the terrain). In cases where holes remained in the model, the mesh was hand built to match the recognized topography. The furthest back crack of the potential

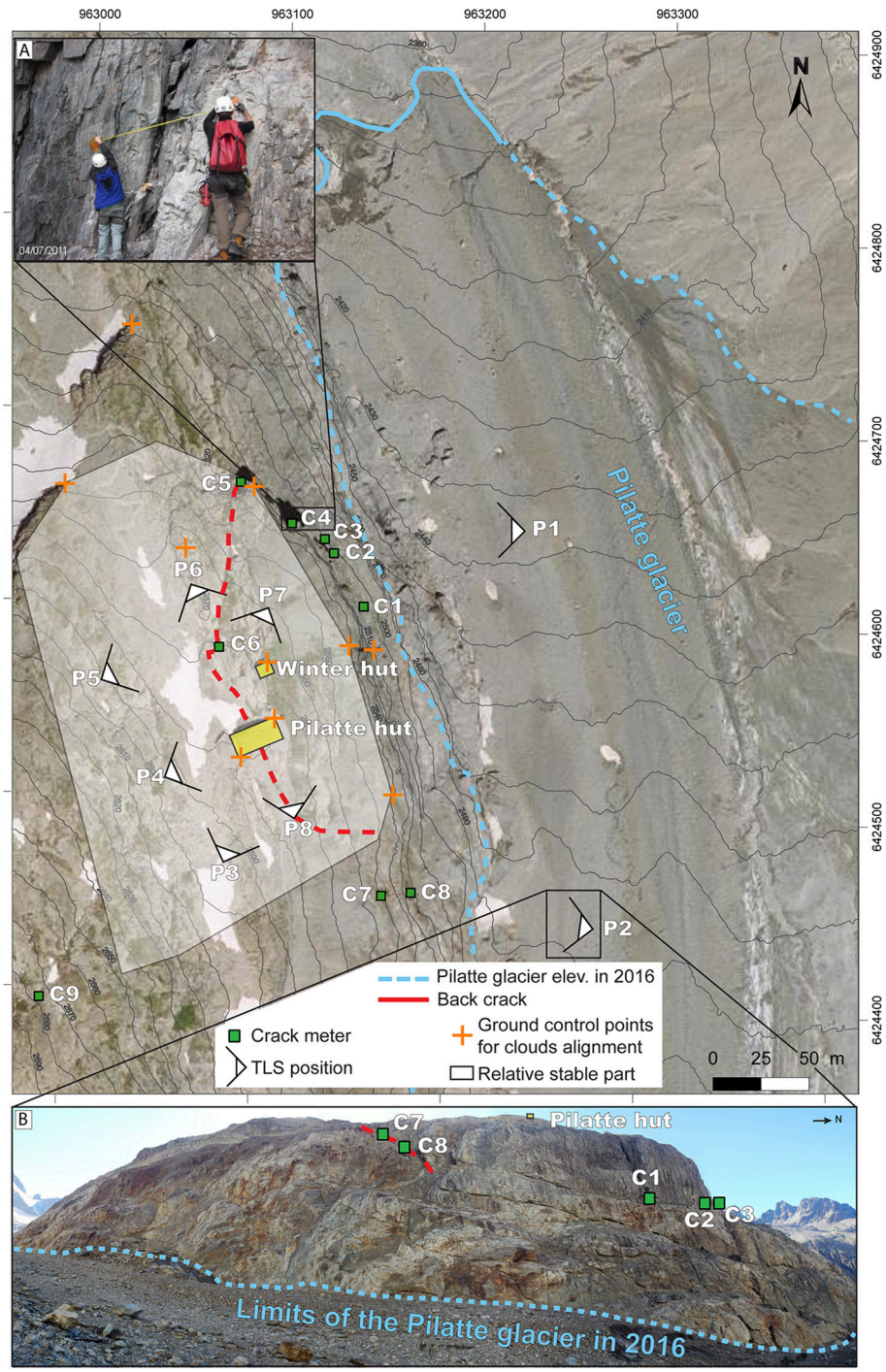

FIGURE 3 | Crack-meter location and TLS survey positions around the Pilatte hut. **(A)** Crack surveying at C4. **(B)** The rock slope below the Pilatte hut from P2 (July 2016).

sliding rock mass was defined by intersecting the main fractures planes. The zones most poorly covered by TLS, which were also interpolated during the meshing process, were not taken into account during the volume computation because they were situated outside of it.

Aerial SfM Photogrammetry

SfM photogrammetry allowed us to measure changes in thickness in the Pilatte glacier over the last few decades from historical aerial photographs. This method has recently become popular (Kappas, 2011; Marcer et al., 2017b; Vargo

et al., 2017; Fugazza et al., 2018). Some other studies have combined terrestrial photogrammetry and TLS data for the reconstruction of detached rock volumes in high mountain environments (Curtaz et al., 2014; Guerin et al., 2017).

The workflow described by Smith et al. (2016) and applied by Guerin et al. (2017) was used to generate point clouds of the glacier and the rockwall beneath the hut for different years with *Agisoft* PhotoScan 1.2.6. and aerial photos obtained from the *Institut Géographique National* (IGN) for the period 1960–2009. The different steps of the workflow are summed up in **Figure 4**. Snow and cloud free aerial images were aligned to create large 3D models of the upper Pilatte basin (**Table 1**). SfM point clouds were generated through 2 main procedures: (1) the alignment of the images according to the camera view points and 6 ground markers which had not been georeferenced, (2) the building of large dense point clouds. The different SfM point clouds were then cut out and only those of the study area were retained (Pilatte hut area with a *c.* 10 m-strip of glacier). These were scaled/aligned with CloudCompare on the 2016 georeferenced TLS point cloud by selecting around 10 pairs of points on each model. Then, to ensure that the clouds were perfectly aligned, each SfM model was cut out between the likely stable part of the rock slope (i.e., no major geometric changes compared to glacier evolution) and the glacier strip. Finally, the stable part was aligned and scaled to the 2016 TLS point cloud using the ICP algorithms (Besl and McKay, 1992).

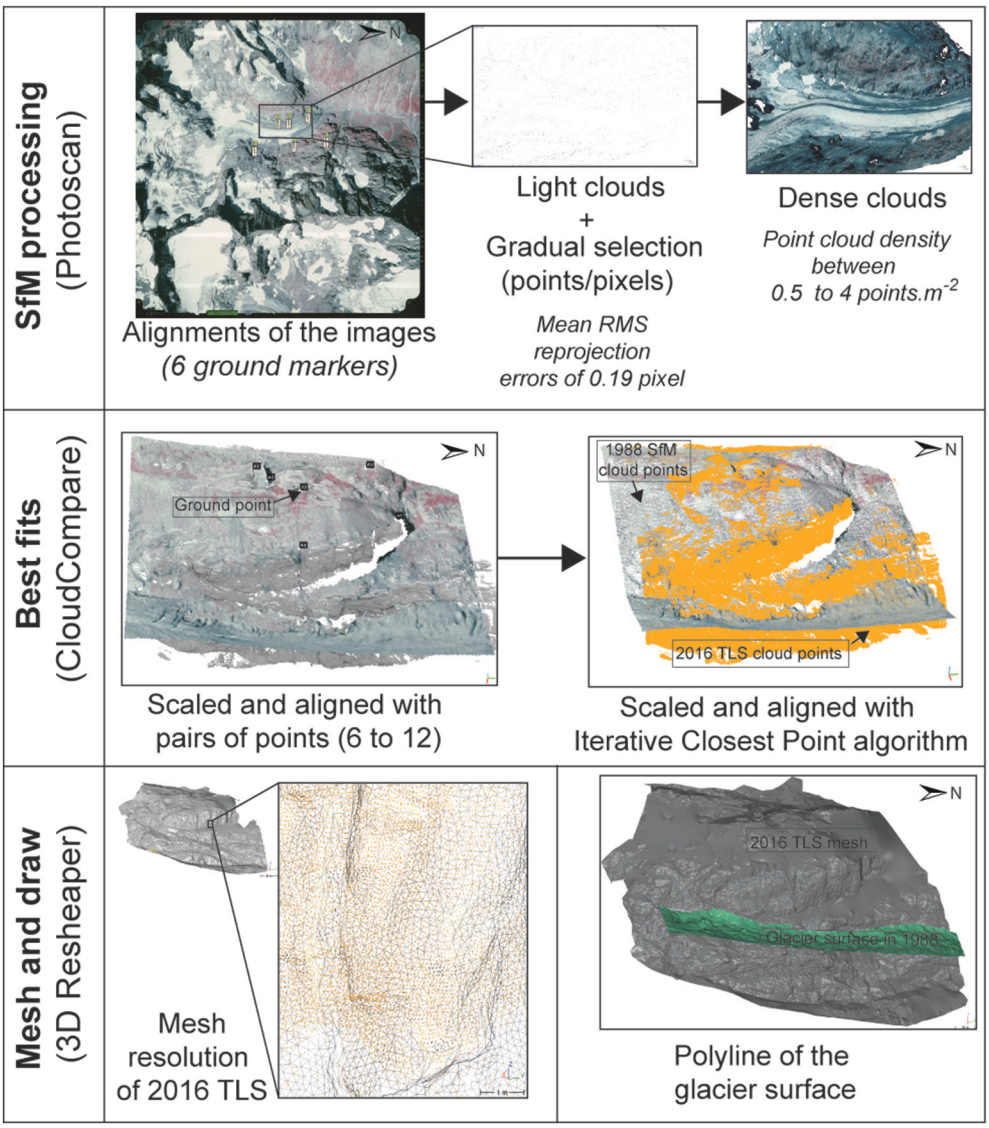

FIGURE 4 | Work flow of the SfM and TLS processing procedures, from the creation of point clouds to the drawing of polylines on the glacier surface (example with 1988 image).

TABLE 1 | Data sets used to generate point clouds by SfM and TLS for the period 1960–2016.

Data	Dates	N pixels/m^2*	N images used	Image type**	N windows	Point density (points/m^2)	N points × 10^3***	Average distance alignment**** (m)
Aerial images	22 Aug. 1960	1.1	6	BW	–	1	36	3
	27 Sept. 1967	1	5	BW	–	0.5	18	2.3
	29 Jul.1981	3.1	9	NIR	–	2.1	103	3.4
	10 Jul. 1988	2.3	6	BW	–	0.7	21	1.3
	15 Aug.1994	3.5	5	NIR	–	1.6	66	1.3
	1 Aug. 2003	3.5	6	RGB	–	1.5	59	2.9
	5 Aug. 2009	11.1	3	RGB	–	3.9	206	1.1
TLS	14 Jul. 2014	–	–	–	8	726	2,105	0.3
	26 Aug. 2016	–	–	–	37	1,272	20,106	–

*N pixels for the same study area centred on the hut.
**BW, black-and white; RGB, red, green, blue (color); NIR, near infrared.
***N points for the same study area centred on the hut.
****Point cloud reference for alignment was the 2016 TLS model.

Aligning and scaling each part independently compensated for the fact that no ground control points had been directly provided for PhotoScan. The 3D model from 2009 was used as the base on which the other models were aligned because of its high resolution and matching of the 2016 TLS point cloud. Polylines representing the contact level between the glacier surface and the rock wall from 1960 to 2009 were generated from SfM point clouds drawn onto the 2016 TLS model, and completed with the 2014 TLS point cloud.

RESULTS

Structural Analysis and Crack Dynamics

Using the on-site mapping of the main cracks and the 2016 point cloud, three main discontinuity groups were identified as delineating the unstable rock mass (**Figure 5**): (i) a series of cracks at the back, crossing the hut and varying between 145-160/50 (dip direction/dip angle) and, very locally in the lower part of the rock mass, 110/50 to 145-160/30; (ii) two basal sliding planes in series (145-160/25-30); (iii) in addition, the unstable rock mass is sub-horizontally divided into two sections (an upper and a lower mass). The upper one is also cut by four sub-vertical fractures.

Based on the structural data, we chose the positions of the crack-meters in order to optimize our understanding of the mechanism of the rock mass movement. The upper rock mass was surveyed each year with one crack-meter placed at the Pilatte hut since 2003, and with four more crack-meters since 2009 or 2011 (**Table 2**). During the two last decades, the back cracks have been very active, ranging from an increase in width of 2–3 mm at the north end (C5) since 2009 to 9 mm on the upper part (C6) since 2003. A very significant increase in width occurred at the beginning of Summer 2008, with a +2–4 mm increase in the back crack near the hut (C6), and also inside the hut between April and the end of June (**Figure 6**). Then, probably between September 2012 and August 2013, a contraction and probably a small rotation toward the south of at least the upper rock mass occurred in connection with the closing movement of four sub-vertical cracks (C1, C2, C3, and C4) and also the closing movement of the southern crack (C8).

Volume of the Unstable Rock Mass and Rockfall Activity

Based on fault-lines which have been identified in the field and which individualize the unstable mass, and particularly on two possible rock slope sliding planes (see **Figure 5**), the geometry of the rock mass can be described as a polyhedron of 90 × 184 × 24 m (height × width × thickness) for a volume comprised between 323,000 m^3 (upper rock mass) and 392,000 m^3 (upper and lower rock masses) ±5–10%.

By comparing the 3D models of 2014 and 2016, one single rockfall was identified in massive polished rock just under the lower basal sliding plane, with a volume of 22.3 ± 1.5 m^3 (**Figure 5D**; 2.3 × 9 × 1 m). No event in the unstable rock mass was detected. In any case, given the fracture measurements and the scale of the terrain measured, movement would not have been detectable due to uncertainty in the TLS measurements. Only rockfalls with a depth greater than 25 cm could be confirmed. Less significant changes might be due to errors in TLS point cloud alignment rather than rockfall events.

Evolution of the Level of the Pilatte Glacier Surface

The thickness of the Pilatte glacier at the foot of the hut has decreased by 155 m since the end of the LIA and by 66 m between 1960 and 2016 (**Figure 7**). The glacier surface lowered by *c.* −22 ± 5 m between 1960 and 1967, then increased in thickness by *c.* 18 ± 4 m over the 1967–1988 period. Since 1988, the surface lowering has accelerated: *c* −23 ± 1 m from 1988 to 2003 and *c.* −39 ± 3 m from 2003 to 2016.

DISCUSSION

Potential Active Triggering Processes

Four major factors, which may combine, can trigger rockfalls and deep-seated rockslides in high mountain areas: seismic

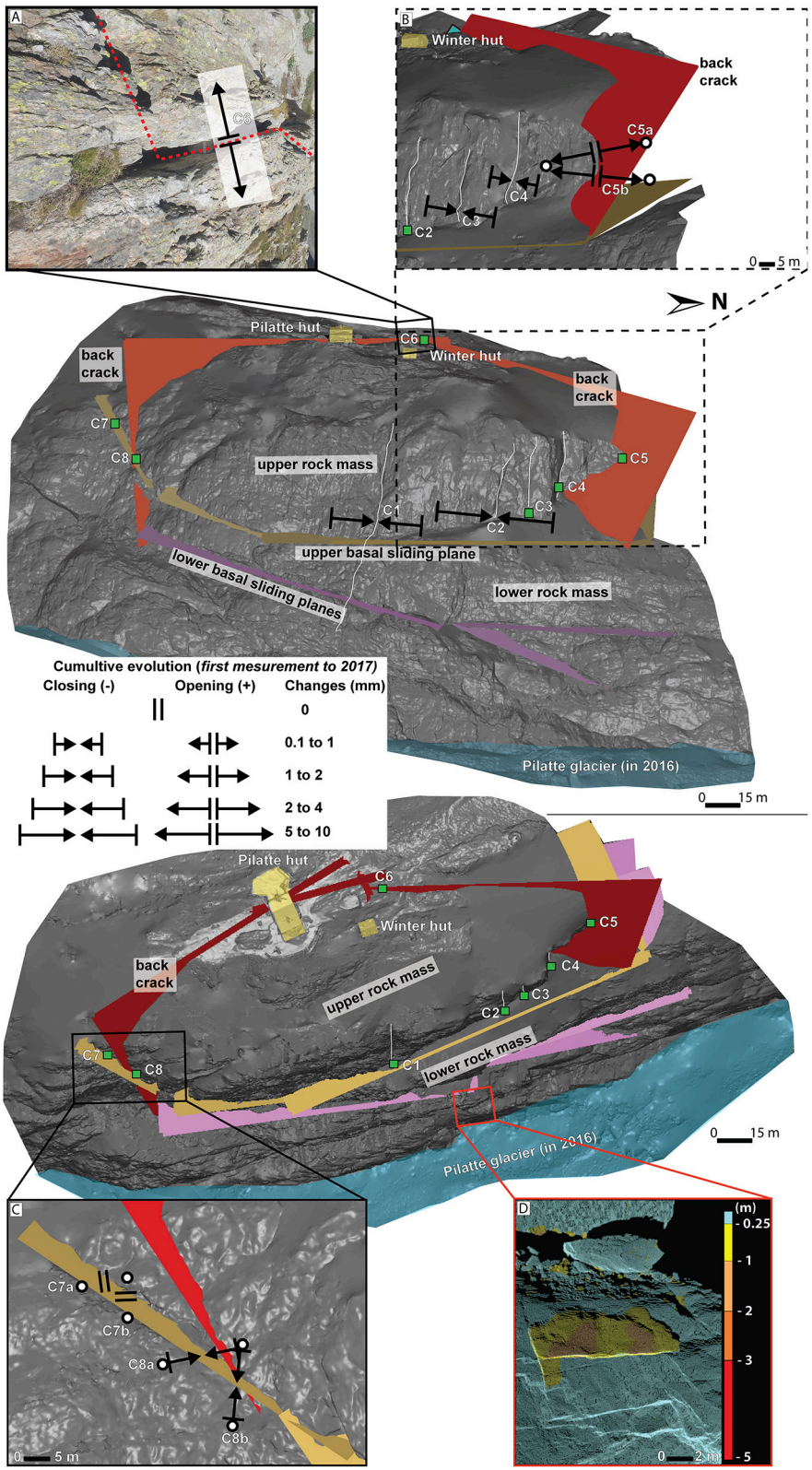

FIGURE 5 | Delimitation of the unstable rock mass and evolution of the monitored fracture lines over the period 2011–2017. View from the glacier **(A,B)** and aerial view **(C,D)**. D: rockfall detected when comparing the TLS 3D models of 2014 and 2016.

TABLE 2 | Cumulative movement monitored by crack-meters.

	Crack-meter deviation from the first measurement* (mm)										
Dates	**C1**	**C2**	**C3**	**C4**	**C5a**	**C5b**	**C6****	**C7a**	**C7b**	**C8a**	**C8b**
Sept. 2003											
Sept. 2004							0.5				
Sept. 2005							0.7				
Sept. 2006							0.3				
Aug. 2007							1.2				
Sept. 2008							7.2				
Aug. 2009							6.4				
Aug. 2010				–	–	–	7.0	–	–		
Jul. 2011				1	0	0	-	1	1		
Aug. 2011	−1	−3	−2	2	1	4	7.3	2	0	3	5
Jul. 2012	2	−1	−3	3	3	3	–	3	2	4	4
Sept. 2012	3	−1	−3	2	2	2	7.7	3	3	3	4
Aug. 2013	0	−6	−5	−1	4	2	8.2	0	2	1	0
Aug. 2014	0	−4	−3	−1	3	2	8.5	3	2	–	–
Jul. 2015	−1	−4	−3	−3	3	3	8.0	0	1	0	0
Jun. 2016	−2	−4	−3	−2	2	0	9.2	1	1	0	−1
Jul. 2017	−4	−6	−2	−1	2	3	9.6	0	0	−2	−2

In black: set up of the measurement system.
***Vernier caliper with mm precision.*

activity (Keefer, 2002; Jibson et al., 2004; Kargel et al., 2015), warming permafrost (Gruber and Haeberli, 2007; Harris et al., 2009; Ravanel et al., 2017), glacial debuttressing due to glacier retreat (Ballantyne, 2002; Hewitt, 2004; Dadson and Church, 2005; Oppikofer et al., 2008; McColl, 2012), and the influence of water flow from rainfall or meltwater (Krautblatter et al., 2013; Draebing et al., 2014, 2017).

Seismicity cannot be considered a triggering factor for destabilization in this study. The seismicity observation network in the French Alps (SISMalp) did not record any significant earthquakes in the Écrins massif in the first half of 2008, the period corresponding to the main recent acceleration of destabilization. Moreover, no event greater than 3 on the Richter scale was recorded during the period 1950–2018. As the study site is not located within the permafrost zone, its warming and the corresponding degradation of interstitial ice cannot either be considered a trigger for destabilization. The role of seasonal ice can also be rejected given the likely depth (up to 35 m) of the detached material. It is unlikely that negative temperatures would occur deep enough within the rock mass to produce seasonal ice capable of exerting sufficient pressure (see Matsuoka and Murton, 2008). Another triggering factor, the influence of water (rainfall, snow melt) on slope stability, is usually modeled as pressure exerted by water which partially fills the joints (Hoek and Bray, 1981). This process requires watertight joints so that the water level can rise. At the Pilatte hut, this situation seems improbable because the visible rock joints are abundant and therefore likely to be sufficiently permeable to allow natural drainage in the rock mass. It is also very unlikely that the glacier constituted an aquiclude, as the Pilatte glacier is not cold but temperate and sliding (Lliboutry et al., 1976; Suter et al., 2001). In such a configuration, there is generally a more or less discontinuous space—known as randkluft—between the ice and the rock.

Therefore, glacial debuttressing appears to be the most likely candidate for triggering rock slope instability beneath the Pilatte hut due to glacial retreat over recent decades. The hut, located between the stable rock slope and an unstable rock mass, would inevitably suffer the consequences of a downslope movement of the latter in paraglacial conditions (McColl, 2012).

Timing of the Glacier Surface Lowering and Dynamics of the Rock Mass

In 1960, the glacier surface was located a few meters downhill from the upper rock mass, but by 1967 it had lowered to a level which was below the lower rock mass (**Figure 8**). In 1981, the glacier surface was located slightly higher, only just beneath the lower rock mass, which possibly constitutes part of the zone which has shifted. By 1988, the glacier level was much higher, approximately at mid-height of the lower rock mass. This was at the end of a period of growth and the glacier likely applied strong pressure to the slope (Cossart et al., 2008, 2013). Indeed, it is at this time that damage to the hut was first observed (1985–1990). From the mid-1970s to late 1980s, alpine glacier thicknesses and lengths increased due to high winter accumulation and reduced summer ablation (Vincent, 2002).

With the ensuing retreat (−63 m in thickness between 1988 and 2016), pressures were reversed, thus decompressing the lower rock mass which, as a result, likely generated the displacement of the entire mass of rock. As such the hypothesis that it was the lower sliding plane that determined the movement of the rock mass rather than the upper one becomes more plausible. This is reinforced by the observations made in the field that show no evidence of movement at the level of the upper plane while many signs indicate movement on the lower one (changes in volume measured by TLS, visible rock fall scars, recent debris observed on the glacier, presence of overhangs, etc.). The most serious damage to the hut occurred in the 1990s, culminating in 2008 with the most active opening period of the back crack.

Within the complex geomorphological history of the slope, the first destructive events affecting the hut would have started with the compression of the rock mass by the glacier, perhaps combined with a slight rotation toward the north, i.e., in the direction of flow of the glacier. In recent times, however, with the retreat of the glacier, the slope has undergone mechanical decompression (Oppikofer et al., 2008; Kos et al., 2016). As indicated by the extensometric measurements, the unstable rock mass has shifted downhill, associated with a probable rotation toward the south.

Unfortunately, the lower sliding plane was not monitored, but the movement probably originated in this zone. It would also have been interesting to monitor possible relative movements between the upper and the lower rock masses.

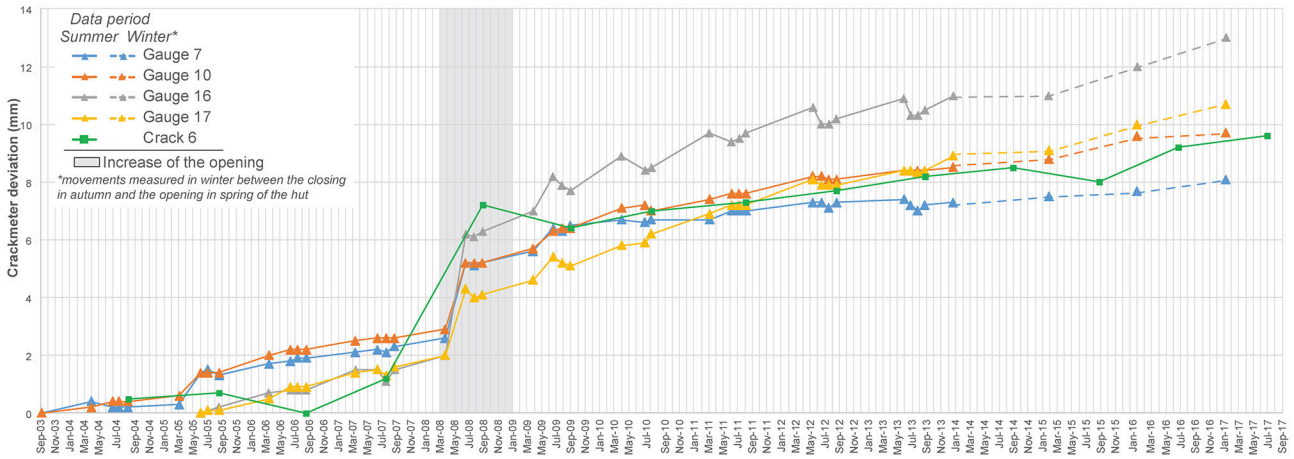

FIGURE 6 | *Saugnac* gauge measurements showing the evolution of the cracks since 2003 (gauges 7–10) or 2005 (gauges 16–17) inside the Pilatte hut, and of the main crack north of the hut measured with a crack-meter (crack 6).

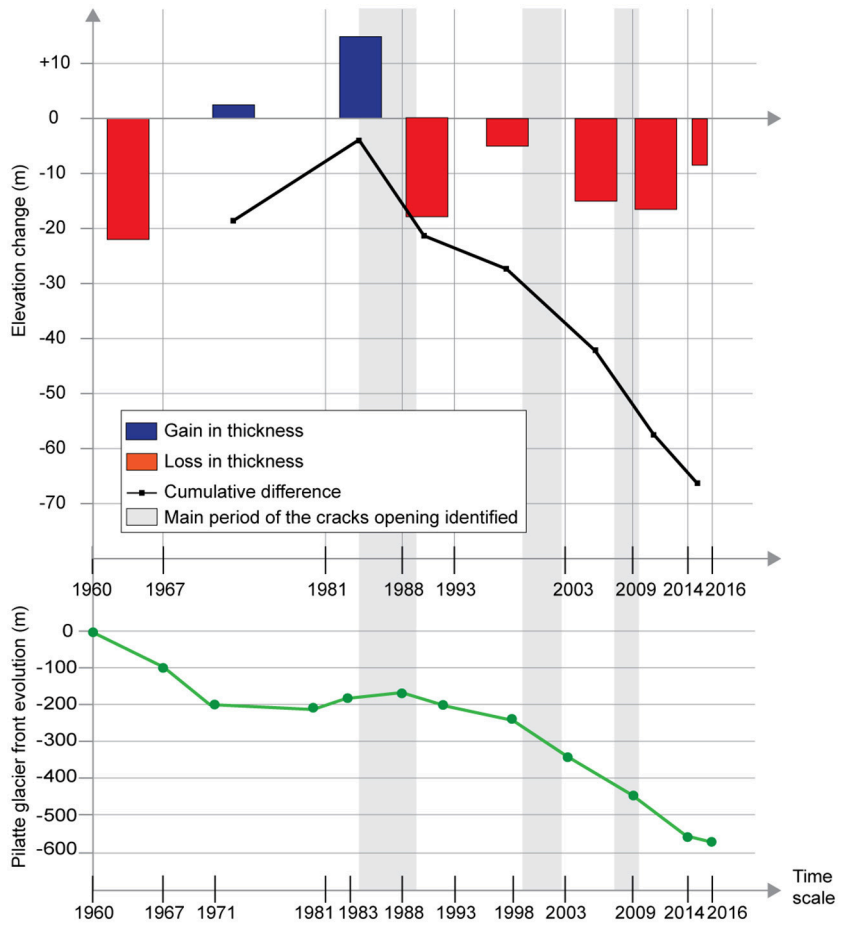

FIGURE 7 | Glacier surface evolution downstream from the Pilatte rock slope, and retreat of the Pilatte glacier over 8 (level) to 11 (front) periods between 1960 and 2016. The three images of 1967, 1983, and 1998 were only used for measuring the glacier front retreat, not for generating 3D point clouds because of snow or clouds during acquisition.

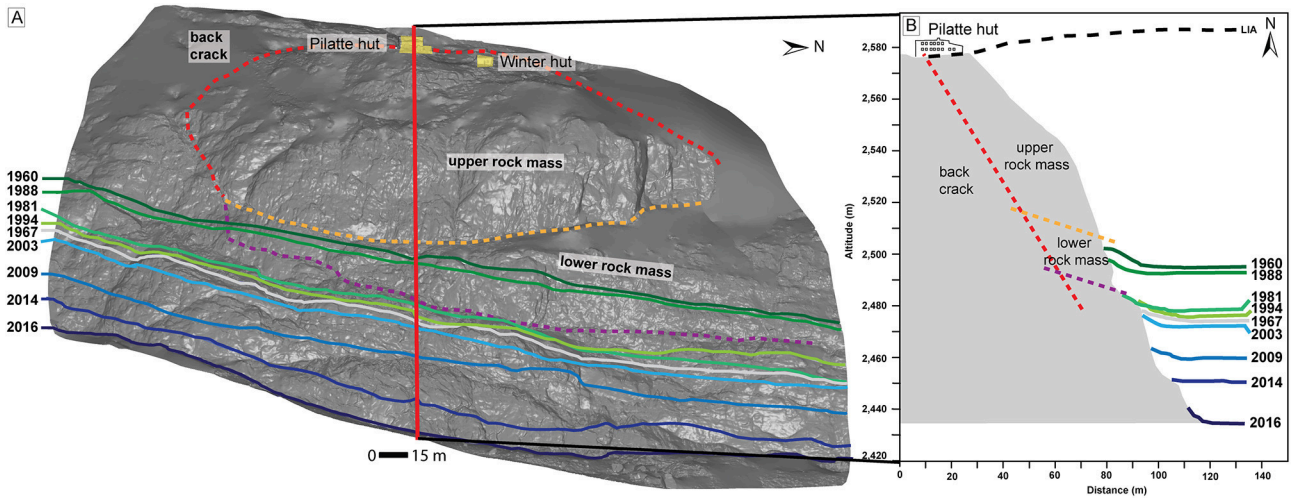

FIGURE 8 | Surface level changes of the Pilatte glacier from 1960 to 2016. These were reconstructed from SfM and TLS analysis and superimposed on the 2016 meshed point cloud. **(A)** View from the glacier. **(B)** Profile of the rock slippage zone at the foot of the Pilatte hut; sliding planes are probably inactive at the base of the upper rock mass (orange dotted line) while they are probably active at the base of the lower rock mass (purple dotted line).

Since 2010, low geomorphological activity suggests a relative stabilization of the mountainside. Despite the difficulty in interpreting information from the LIA and the recent deglaciations, the Pilatte rock slippage seems to have occurred almost immediately after the onset of the paraglacial period (decennial scale) described by Ballantyne (2002): "rapid paraglacial rockwall retreat due to stress release, joint propagation and consequent rockfall immediately after deglaciation, with progressive reduction of rockfall activity as the cliff regains stability."

CONCLUSIONS AND OUTLOOKS

Detailed documentation of paraglacial movements is quite rare, and even more so in cases where they have affected infrastructure. The Pilatte glacier thickness was locally reconstructed with historical imagery for the period 1960–2009 by SfM in order to review possible paraglacial rock slope control, while crack width was monitored inside the hut and outside on the unstable rock mass. Despite the fact that the monitoring of this rock slippage started after its largest known movement, it has helped in understanding the dynamics: a rock mass of 392,000 m^3 would have been compressed during the last glacier advance of the 1980s before undergoing debuttressing due to the rapid retreat of the Pilatte glacier over the past decades. The initiation and the continued development of the rock slope failure along a sliding plane occurred less than 10 years after the glacier surface started lowering in the 1980s. This paraglacial rock slope adjustment, the understanding of which has been facilitated by the presence of the hut, illustrates the first theoretical decennial dynamics of a paraglacial period.

This study used extensometric data from methods that have variable and sometimes significant uncertainties. Moreover, some of these were incorrectly carried out (e.g., data from the annual crack-meter survey is less authoritative because some years are missing). The low amplitude of crack opening since 2010, as well as the low geomorphological activity monitored by TLS, suggest an ongoing (but temporary?) stabilization of the mountainside. Although the paraglacial dynamics highlighted in this study seem to be have diminished, it will be necessary to continue monitoring the cracks and the rock slope in order to study its evolution, and possibly to constitute an early warning system in case of rock slope failure.

AUTHOR CONTRIBUTIONS

P-AD and LR designed research and conducted TLS field investigations and SfM workflow. P-AD prepared data, made all figures and wrote the initial version of the paper under the supervision of LR. LR and PD improved the manuscript. LD conducted cracks surveys since 2009.

ACKNOWLEDGMENTS

P-AD PhD fellowship is supported by a grant from *Ingenierie des Mouvements du Sol et des Risques Naturels* (IMSRN) and the *Association Nationale de la Recherche et de la Technologie* (ANRt). Authors thank K. Ayroles, M. Marcer, and J. Mourey for their help in carrying the TLS. We also thank K. Génuite for SfM processing assistance and his personal insight, and the *Fédération Française des Clubs Alpins et de Montagne* and the *Parc National des Écrins* for promoting this study. Finally, we would like to thank the two reviewers for their helpful and critical review. This study is part of FEDER POIA *PermaRisk* project.

REFERENCES

Abellan, A., Derron, M.-H., and Jaboyedoff, M. (2016). "Use of 3D Point Clouds in Geohazards" special issue: current challenges and future trends. *Remote Sens.* 8:130. doi: 10.3390/rs8020130

Ballantyne, C. K. (2002). Paraglacial geomorphology. *Quat. Sci. Rev.* 21, 1935–2017. doi: 10.1016/S0277-3791(02)00005-7

Ballantyne, C. K. (2013). "Paraglacial geomorphology," in *The Encyclopedia of Quaternary Sciences, Vol. 3, 2nd Edn* (Amsterdam: Elsevier), 553–565.

Barféty, J. C., and Pécher, A. (1984). *Notice Explicative de la Carte Géologique n° 822 de Saint-Christophe-en-Oisans à 1/50000*. Orléans: BRGM. Available online at: http://ficheinfoterre.brgm.fr/Notices/0822N.pdf

Beniston, M., Farinotti, D., Stoffel,and M., Andreassen, L. M., Coppola, E., Eckert, N., et al. (2018). The European mountain cryosphere: a review of its current state, trends, and future challenges. *Cryosphere* 12, 759–794. doi: 10.5194/tc-12-759-2018

Besl, P. J., and McKay, N. D. (1992). A method for registration of 3-D shapes. *IEEE Trans. Pattern Anal. Mach. Intell.* 14, 239–256. doi: 10.1109/34.121791

Bhardwaj, A., Sam, L., Bhardwaj, A., and Martín-Torres, F. J. (2016). LiDAR remote sensing of the cryosphere: present applications and future prospects. *Remote Sens. Environ.* 177, 125–143. doi: 10.1016/j.rse.2016.02.031

Blair, R. W. (1994). Moraine and valley wall collapse due to rapid deglaciation in Mount Cook National Park, New Zealand. *Mt. Res. Dev.* 14, 347–358. doi: 10.2307/3673731

Bodin, X., Thibert, E., Sanchez, O., Rabatel, A., and Jaillet, S. (2018). Multi-annual kinematics of an active rock glacier quantified from very high-resolution DEMs: an application-case in the French Alps. *Remote Sens*. 10:547. doi: 10.3390/rs10040547

Church, M., and Ryder, J. M. (1972). Paraglacial sedimentation: a consideration of fluvial processes conditioned by glaciation. *Geol. Soc. Am. Bull.* 83, 3059–3072. doi: 10.1130/0016-7606(1972)83[3059:PSACOF]2.0.CO;2

Cossart, E., Braucher, R., Fort, M., Bourlès, D. L., and Carcaillet, J. (2008). Slope instability in relation to glacial debuttressing in alpine areas (Upper Durance catchment, southeastern France): Evidence from field data and 10Be cosmic ray exposure ages. *Geomorphology* 95, 3–26. doi: 10.1016/j.geomorph.2006.12.022

Cossart, E., Mercier, D., Decaulne, A., and Feuillet, T. (2013). An overview of the consequences of paraglacial landsliding on deglaciated mountain slopes: typology, timing and contribution to cascading fluxes. *Quat. Rev. Assoc. Fr. Pour Létude Quat.* 24, 13–24. doi: 10.4000/quaternaire.6444

Curtaz, M., Ferrero, A. M., Roncella, R., Segalini, A., and Umili, G. (2014). Terrestrial photogrammetry and numerical modelling for the stability analysis of rock slopes in high mountain areas: aiguilles marbrées case. *Rock Mech. Rock Eng.* 47, 605–620. doi: 10.1007/s00603-013-0446-z

Dadson, S. J., and Church, M. (2005). Postglacial topographic evolution of glaciated valleys: a stochastic landscape evolution model. *Earth Surf Processes Landforms* 30, 1387–1403. doi: 10.1002/esp.1199

Deline, P., Gardent, M., Magnin, F., and Ravanel, L. (2012). The morphodynamics of the mont blanc massif in a changing cryosphere: a comprehensive review. *Geogr. Ann. Ser. Phys. Geogr.* 94, 265–283. doi: 10.1111/j.1468-0459.2012.00467.x

Delunel, R. (2010). *Evolution géomorphologique du massif des Ecrins-Pelvoux depuis le Dernier Maximum Glaciaire – Apports des nucléides cosmogéniques produits in-situ*. PhD thesis, Université Joseph-Fourier, Grenoble.

Derron, M. H., Jaboyedoff, M., Pedrazzini, A., Michoud, C., and Villemin, T. (2013). "Remote sensing and monitoring techniques for the characterization of rock mass deformation and change detection," in *Rockfall Engineering*, eds S. Lambert and F. Nicot (Wiley-Blackwell), 39–65. doi: 10.1002/9781118601532.ch2

Draebing, D., Krautblatter, M., and Dikau, R. (2014). Interaction of thermal and mechanical processes in steep permafrost rock walls: a conceptual approach. *Geomorphology* 226, 226–235. doi: 10.1016/j.geomorph.2014.08.009

Draebing, D., Krautblatter, M., and Hoffmann, T. (2017). Thermo-cryogenic controls of fracture kinematics in permafrost rockwalls. *Geophys. Res. Lett.* 44, 3535–3544, doi: 10.1002/2016GL072050

Duvillard, P. A., Ravanel, L., and Deline, P. (2015). Risk assessment of infrastructure destabilisation due to global warming in the high French Alps. *J. Alp. Res.* doi: 10.4000/rga.2896

Einhorn, B., Eckert, N., Chaix, C., Ravanel, L., Deline, P., Gardent, M., et al. (2015). Climate change and natural hazards in the Alps. *J. Alp. Res.* doi: 10.4000/rga.2878

Fugazza, D., Scaioni, M., Corti, M., D'Agata, C., Azzoni, R. S., Cernuschi, M., et al. (2018). Combination of UAV and terrestrial photogrammetry to assess rapid glacier evolution and map glacier hazards. *Nat. Hazards Earth Syst. Sci.* 18, 1055–1071. doi: 10.5194/nhess-18-1055-2018

Gardent, M., Rabatel, A., Dedieu, J. P., and Deline, P. (2014). Multitemporal glacier inventory of the French Alps from the late 1960s to the late 2000s. *Glob. Planet. Change* 120, 24–37. doi: 10.1016/j.gloplacha.2014.05.004

Gilbert, A., and Vincent, C. (2013). Atmospheric temperature changes over the 20th century at very high elevations in the European Alps from englacial temperatures. *Geophys. Res. Lett.* 40, 2102–2108. doi: 10.1002/grl.50401

Girardeau-Montaut, D. (2006). *Détection de Changement sur des Données Géométriques Tridimensionnelles*. PhD thesis, Télécom ParisTech.

Grämiger, L. M., Moore, J. R., Gischig, V. S., Ivy-Ochs, S., and Loew, S. (2017). Beyond debuttressing: mechanics of paraglacial rock slope damage during repeat glacial cycles. *J. Geophys. Res. Earth Surf.* 122, 1004–1036. doi: 10.1002/2016JF003967

Gruber, S., and Haeberli, W. (2007). Permafrost in steep bedrock slopes and its temperature-related destabilization following climate change. *J Geophys Res.* 112:F02S18. doi: 10.1029/2006JF000547

Guerin, A., Abellán, A., Matasci, B., Jaboyedoff, M., Derron, M. H., and Ravanel, L. (2017). Brief communication: 3-D reconstruction of a collapsed rock pillar from Web-retrieved images and terrestrial lidar data – the 2005 event of the west face of the Drus (Mont Blanc massif). *Nat. Hazards Earth Syst. Sci.* 17, 1207–1220. doi: 10.5194/nhess-17-1207-2017

Haeberli, W., Wegmann, M., and Vonder Mühll, D. (1997). Slope stability problems related to glacier shrinkage and permafrost degradation in the Alps. *Eclogae Geol. Helvetiae* 90, 407–414. doi: 10.5169/seals-168172

Harris, C., Arenson, L. U., Christiansen, H. H., Etzelmüller, B., Frauenfelder, R., Gruber, S., et al. (2009). Permafrost and climate in Europe: monitoring and modelling thermal, geomorphological and geotechnical responses. *Earth Sci. Rev.* 92, 117–171. doi: 10.1016/j.earscirev.2008.12.002

Hewitt, K. (2004). "Geomorphic hazards in mountain environments," in *Mountain Geomorphology,* eds P. Owens and O. Slaymaker (London: Hodder Scientific), 187–218.

Hoek, E., and Bray, J. W. (1981). *Rock Slope Engineering.* London: Institution Mining Metallurg.

Huggel, C., Zgraggen-Oswald, S., Haeberli, W., Kääb, A., Polkvoj, A., Galushkin, I., et al. (2005). The 2002 rock/ice avalanche at Kolka/Karmadon, Russian Caucasus: assessment of extraordinary avalanche formation and mobility, and application of QuickBird satellite imagery. *Nat. Hazards Earth Syst. Sci.* 5, 173–187. doi: 10.5194/nhess-5-173-2005

Huss, M. (2012). Extrapolating glacier mass balance to the mountain-range scale: the European Alps 1900–2100. *Cryosphere* 6, 713–727. doi: 10.5194/tc-6-713-2012

Jaboyedoff, M., Oppikofer, T., Abellán, A., Derron, M.-H., Loye, A., Metzger, R., et al. (2012). Use of LIDAR in landslide investigations: a review. *Nat. Hazards* 61, 5–28. doi: 10.1007/s11069-010-9634-2

Jibson, R. W., Harp, E. L., Schulz, W., and Keefer, D. K. (2004). Landslides triggered by the 2002 Denali fault, Alaska, earthquake and the inferred nature of the strong shaking. *Earthquake Spectra* 20, 669–691. doi: 10.1193/1.1778173

Kääb, A., Huggel, C., Fischer, L., Guex, S., Paul, F., Roer, I., et al. (2005). Remote sensing of glacier-and permafrost-related hazards in high mountains: an overview. *Nat. Hazards Earth Syst. Sci.* 5, 527–554. doi: 10.5194/nhess-5-527-2005

Kappas, M. (2011). "Aerial photogrammetry for glacial monitoring," in *Encyclopedia of Snow, Ice and Glaciers. Encyclopedia of Earth Sciences Series,* eds V. P. Singh, P. Singh, and U. K. Haritashya (Dordrecht: Springer), 4–15. doi: 10.1007/978-90-481-2642-2

Kargel, J. S., Leonard, G. J., Shugar, D. H., Haritashya, U. K., Bevington, A., Fielding, E. J., et al. (2015). Geomorphic and geologic controls of geohazards induced by Nepal's 2015 Gorkha earthquake. *Science* 351:6269. doi: 10.1126/science.aac8353

Keefer, D. K. (2002). Investigating landslides caused by earthquakes - A historical review. *Surv Geophys.* 23, 473–510. doi: 10.1023/A:1021274710840

Kenner, R., Phillips, M., Danioth, C., Denier, C., Thee, P., and Zgraggen, A. (2011). Investigation of rock and ice loss in a recently deglaciated mountain rock wall using terrestrial laser scanning: Gemsstock, Swiss Alps. *Cold Reg. Sci. Technol.* 67, 157–164. doi: 10.1016/j.coldregions.2011.04.006

Keuschnig, M., Hartmeyer, I., Höfer-Öllinger, G., Schober, A., Krautblatter, M., and Schrott, L. (2015). "Permafrost-Related Mass Movements: Implications from a Rock Slide at the Kitzsteinhorn, Austria," in *Engineering Geology for Society and Territory,* Vol. 1, *Climate Change and Engineering Geology*, eds G. Lollino, A. Manconi, J. Clague, W. Shan, and M. Chiarle (Cham: Springer International Publishing), 255–259.

Kos, A., Amann, F., Strozzi, T., Delaloye, R., von Ruette, J., and Springman, S. (2016). Contemporary glacier retreat triggers a rapid landslide response, Great Aletsch Glacier, Switzerland. *Geophys. Res. Lett.* 43:2016GL071708. doi: 10.1002/2016GL071708

Krautblatter, M., Funk, D., and Günzel, F. K. (2013). Why permafrost rocks become unstable: a rock–ice-mechanical model in time and space. *Earth Surf. Process. Landf.* 38, 876–887. doi: 10.1002/esp.3374

Krautblatter, M., and Leith, K. (2015). "Glacier- and permafrost-related slope instabilities," in *The High-Mountain Cryosphere: Environmental Changes and Human Risks*, eds A. Kääb, C. Huggel, J. J. Clague, and M. Carey (Cambridge: Cambridge University Press), 147–165. doi: 10.1017/CBO9781107588653.009

Le Fort, P. (1971). *Géologie du Haut-Dauphiné cristallin (Alpes Française): Etudes pétrologique et structurale de la partie occidentale*. PhD thesis, Université Nancy.

Lliboutry, L., Briat, M., Creseveur, M., and Pourchet, M. (1976). 15m Deep Temperatures in the Glaciers of Mont Blanc (French Alps). *J. Glaciol.* 16, 197–203. doi: 10.3189/S0022143000031531

Marcer, M., Bodin, X., Brenning, A., Schoeneich, P., Charvet, R., and Gottardi, F. (2017a). Permafrost Favorability Index: Spatial Modeling in the French Alps Using a Rock Glacier Inventory. *Front. Earth Sci.* 5:105. doi: 10.3389/feart.2017.00105

Marcer, M., Stentoft, P. A., Bjerre, E., Cimoli, E., Bjørk, A., Stenseng, L., et al. (2017b). Three decades of volume change of a small greenlandic glacier using ground penetrating radar, structure from motion, and aerial photogrammetry. *Arct. Antarct. Alp. Res.* 49, 411–425. doi: 10.1657/AAAR0016-049

Matsuoka, N., and Murton, J. (2008). Frost weathering recent advances and future directions. *Permafr. Periglac. Process.* 19,195–210. doi: 10.1002/ppp.620

McColl, S. T. (2012). Paraglacial rock-slope stability. *Geomorphology* 153–154, 1–16. doi: 10.1016/j.geomorph.2012.02.015

McColl, S. T., and Davies, T. R. H. (2013). Large ice-contact slope movements: glacial buttressing, deformation and erosion. *Earth Surf. Process. Landf.* 38, 1102–1115. doi: 10.1002/esp.3346

Mercier, D. (2008). Paraglacial and paraperiglacial landsystems: concepts, temporal scales and spatial distribution. *Géomorphol. Relief Process. Environ.* 14, 223–233. doi: 10.4000/geomorphologie.7396

Mercier, D. (2010). *La géomorphologie Paraglaciaire. Analyse de Crises érosives d'origine Climatique Dans les Environnements Englacés et sur Leurs Marges*. HDR thesis, Université Blaise Pascal, Clermont-Ferrand II.

Mourey, J., and Ravanel, L. (2017). Evolution of access routes to high mountain refuges of the Mer de Glace Basin (Mont Blanc Massif, France). *J. Alp. Res.* doi: 10.4000/rga.3780

Nordvik, T., Blikra, L. H., Nyrnes, E., and Derron, M.-H. (2010). Statistical analysis of seasonal displacements at the Nordnes rockslide, northern Norway. *Eng. Geol.* 114, 228–237. doi: 10.1016/j.enggeo.2010.04.019

O'Connor, J. E., and Costa, J. E. (1993). Geologic and hydrologic hazards in glacierized basins in North America resulting from 19th and 20th century global warming. *Nat. Hazards* 8, 121–140. doi: 10.1007/BF00605437

Oppikofer, T., Jaboyedoff, M., Blikra, L., Derron, M.-H., and Metzger, R. (2009). Characterization and monitoring of the Åknes rockslide using terrestrial laser scanning. *Nat. Hazards Earth Syst. Sci.* 9, 1003–1019. doi: 10.5194/nhess-9-1003-2009

Oppikofer, T., Jaboyedoff, M., and Keusen, H.-R. (2008). Collapse at the eastern Eiger flank in the Swiss Alps. *Nat. Geosci.* 1, ngeo258. doi: 10.1038/ngeo258

Petley, D. (2017). *Murchison Hut: An Interesting Landslide Problem in Aoraki/Mount Cook National Park*. The Landslide Blog. Available online at: https://blogs.agu.org/landslideblog/2017/10/03/murchison-hut-1/

PERMOS (2016). "Permafrost in Switzerland 2010/2011 to 2013/2014," in *Glaciological Report (Permafrost) No. 12-15 of the Cryospheric Commission of the Swiss Academy of Sciences*, eds J. Noetzli, R. Luethi, and B. Staub (Fribourg), 85.

Pomerleau, F., Colas, F., Siegwart, R., and Magnenat, S. (2013). Comparing ICP variants on real-world data sets. *Auton. Robots* 34, 133–148. doi: 10.1007/s10514-013-9327-2

Rabatel, A., Dedieu, J. P., and Vincent, C. (2016). Spatio-temporal changes in glacier-wide mass balance quantified by optical remote sensing on 30 glaciers in the French Alps for the period 1983–2014. *J. Glaciol.* 62, 1153–1166. doi: 10.1017/jog.2016.113

Rabatel, A., Deline, P., Jaillet, S., and Ravanel, L. (2008). Rock falls in high-alpine rock walls quantified by terrestrial lidar measurements: a case study in the Mont Blanc area. *Geophys. Res. Lett.* 35:L10502. doi: 10.1029/2008GL033424

Rabatel, A., Letréguilly, A., Dedieu, J.-P., and Eckert, N. (2013). Changes in glacier equilibrium-line altitude in the western Alps from 1984 to 2010: evaluation by remote sensing and modeling of the morpho-topographic and climate controls. *Cryosphere* 7, 1455–1471. doi: 10.5194/tc-7-1455-2013

Ravanel, L., Deline, P., and Bodin, X. (2015a). "LiDAR-Helped Recognition and Promotion of High-Alpine Geomorphosites," in *Engineering Geology for Society and Territory,* Vol. 8, *Preservation of Cultural Heritage*, eds G. Lollino, D. Giordan, C. Marunteanu, B. Christaras, I. Yoshinori, and C. Margottini (Cham: Springer International Publishing), 249–252.

Ravanel, L., Deline, P., Lambiel, C., and Duvillard, P.-A. (2015b). "Stability Monitoring of High Alpine Infrastructure by Terrestrial Laser Scanning," in *Engineering Geology for Society and Territory*, Vol. 1, *Climate Change and Engineering Geology*, eds G. Lollino, A. Manconi, J. Clague, W. Shan, and M. Chiarle (Cham: Springer International Publishing), 169–172. doi: 10.1007/978-3-319-09300-0_32

Ravanel, L., Deline, P., Lambiel, C., and Vincent, C. (2013). Instability of a high alpine rock ridge: the lower arête des cosmiques, mont blanc massif, france. *Geogr. Ann. Ser. Phys. Geogr.* 95, 51–66. doi: 10.1111/geoa.12000

Ravanel, L., Magnin, F., Deline, P. (2017). Impacts of the 2003 and 2015 summer heat waves on permafrost-affected rockwalls in the Mont Blanc massif. *Sci. Total Environ.* 609: 132–143. doi: 10.1016/j.scitotenv.2017.07.055

Ritter, F., Fiebig, M., and Muhar, A. (2012). Impacts of Global Warming on Mountaineering: A Classification of Phenomena Affecting the Alpine Trail Network. *Mt. Res. Dev.* 32, 4–15. doi: 10.1659/MRD-JOURNAL-D-11-00036.1

Slob, S., and Hack, R. (2004). "3D Terrestrial Laser Scanning as a New Field Measurement and Monitoring Technique," in *Engineering Geology for Infrastructure Planning in Europe*, eds R. Hack, R. Azzam, and R. Charlier (Berlin; Heidelberg: Springer), 179–189.

Smith, M. W., Carrivick, J. L., and Quincey, D. J. (2016). Structure from motion photogrammetry in physical geography. *Prog. Phys. Geogr.* 40, 247–275. doi: 10.1177/0309133315615805

Strozzi, T., Delaloye, R., Kääb, A., Ambrosi, C., Perruchoud, E., and Wegmüller, U. (2010). Combined observations of rock mass movements using satellite SAR interferometry, differential GPS, airborne digital photogrammetry, and airborne photography interpretation. *J. Geophys. Res. Earth Surf.* 115:F01014. doi: 10.1029/2009JF001311

Suter, S., Laternser, M., Haeberli, W., Frauenfelder, R., and Hoelzle, M. (2001). Cold firn and ice of high-altitude glaciers in the Alps: measurements and distribution modelling. *J. Glaciol.* 47, 85–96. doi: 10.3189/172756501781832566

Telling, J., Lyda, A., Hartzell, P., and Glennie, C. (2017). Review of Earth science research using terrestrial laser scanning. *Earth Sci. Rev.* 169, 35–68. doi: 10.1016/j.earscirev.2017.04.007

Vargo, L. J., Anderson, B. M., Horgan, H. J., Mackintosh, A. N., Lorrey, A. M., and Thornton, M. (2017). Using structure from motion photogrammetry to measure past glacier changes from historic aerial photographs. *J. Glaciol.* 63, 1105–1118. doi: 10.1017/jog.2017.79

Vincent, C. (2002). Influence of climate change over the 20th Century on four French glacier mass balances. *J. Geophys. Res. Atmospheres* 107, 4375. doi: 10.1029/2001JD000832

Vivian, R., and Bergeret, R. (1967). Le glacier de la Pilatte. *Rev. Géographie Alp.* 55, 392–395. doi: 10.3406/rga.1967.3324

Wieczorek, G. F., and Jäger, S. (1996). Triggering mechanisms and depositional rates of postglacial slope-movement processes in the Yosemite Valley, California. *Geomorphology* 15, 17–31. doi: 10.1016/0169-555X(95)00112-I

Zanoner, T., Carton, A., Seppi, R., Carturan, L., Baroni, C., Salvatore, M. C., et al. (2017). Little Ice Age mapping as a tool for identifying hazard in the paraglacial environment: The case study of Trentino (Eastern Italian Alps). *Geomorphology* 295, 551–562. doi: 10.1016/j.geomorph.2017.08.014

Conflict of Interest Statement: The authors declare that the research was conducted in the absence of any commercial or financial relationships that could be construed as a potential conflict of interest.